



**Acoustics'08
Paris**
June 29-July 4, 2008

www.acoustics08-paris.org

euronoise

A study on regularization parameter choice in Near-field Acoustical Holography

Jesper Gomes^a and Per Christian Hansen^b

^aBrüel & Kjær Sound and Vibration Measurement A/S, Skodsborgvej 307, DK-2850 Nærum, Denmark

^bDTU Informatics, Technical University of Denmark, Building 321, DK-2800 Kgs. Lyngby, Denmark

jgomes@bksv.com

Regularization plays an important role in Near-field Acoustical Holography (NAH), and choosing the right amount of regularization is crucial in order to get a meaningful solution. Automated methods such as the L-curve Criterion (L-C) or Generalized Cross Validation (GCV) are often used in NAH to choose a regularization parameter. These parameter choice methods (PCMs) are attractive, since they require no a priori knowledge about the noise – however, there seems to be no clear understanding of when one PCM is better than the others. This paper presents a comparison of three PCMs: GCV, L-C, and Normalized Cumulative Periodogram (NCP). The latter method is new within NAH, and it is based on the statistical properties of the residual vector. The methods are used in connection with three NAH methods: Statistically Optimized Near-field Acoustical Holography (SONAH), the Inverse Boundary Element Method (IBEM), and the Equivalent Source Method (ESM). All combinations of PCMs and NAH methods are investigated using simulations with different types of noise, and comparisons are also carried out for a practical experiment. The aim of this work is to create a better understanding of which mechanisms affect the performance of the different PCMs.

1 Introduction

Several methods have been developed in the area of Near-field Acoustical Holography (NAH), such as Statistically Optimized Near-field Acoustical Holography (SONAH) [8, 3, 2], the Equivalent Source Method (ESM) [6], and the Inverse Boundary Element Method (IBEM) [1, 7]. In the presence of noise, all these methods require regularization in order to get a meaningful estimation of the acoustic quantities (sound pressure, particle velocity, and/or intensity) on the source surface of interest.

The optimal amount of regularization is unknown in practice, and automated procedures such as Generalized Cross Validation (GCV) or the L-curve criterion (L-C) are often used to select the regularization parameter [4]. The performance of a parameter choice method (PCM) depends on both data and the associated NAH approach. In [9] different PCMs are compared using conventional Fourier based NAH, in [7] the comparisons are based on an indirect IBEM formulation, and in [2] SONAH is investigated with respect to the PCMs.

In this paper, GCV, L-C, and a recently developed method, based on the Normalized Cumulative Periodogram (NCP) [5], are used with SONAH, ESM, and IBEM. The aim is to see how the performance of the PCMs change with the data across the investigated NAH methods, and to get a clearer picture of when to use which PCM. The results are based on Tikhonov regularization only.

2 Brief Outline of Theory

2.1 The Reconstruction Methods

Throughout, \mathbf{r} denotes a general position vector, and \mathbf{r}_i is the position of the i th measurement. The pressure at \mathbf{r} is denoted by $p(\mathbf{r})$, and the vector \mathbf{p} holds the measured data in a set of measurement points. Given $p(\mathbf{r})$, the particle velocity in the direction χ is given by

$$v_\chi(\mathbf{r}) = \frac{-1}{j\omega\rho_0} \frac{\partial p(\mathbf{r})}{\partial \chi}, \quad (1)$$

where ω is the angular frequency, ρ_0 is the density of the medium, and the implicit time variation is $e^{j\omega t}$.

SONAH. In a homogenous and source-free medium, any sound field on one side of an infinite plane can be uniquely expanded into plane and evanescent waves.

Hence we can write the pressure as the inner product of two infinite vectors:

$$p(\mathbf{r}) = \mathbf{a}^T \boldsymbol{\alpha}(\mathbf{r}). \quad (2)$$

Here, $\alpha_j(\mathbf{r})$ is the value of the j th wave component in the plane wave expansion at \mathbf{r} , and a_j is the complex amplitude of that component. The sound pressure at a set of measurement points is then given by

$$\mathbf{p} = \mathbf{A} \mathbf{a}, \quad (3)$$

in which the i th row in \mathbf{A} equals $\boldsymbol{\alpha}(\mathbf{r}_i)^T$.

The coefficients can, e.g., be estimated by solving Eq. (3) in a Tikhonov regularized least squares sense,

$$\mathbf{a}_\lambda = (\mathbf{A}^H \mathbf{A} + \lambda^2 \mathbf{I})^{-1} \mathbf{A}^H \mathbf{p}, \quad (4)$$

where \mathbf{I} is the identity matrix, H denotes Hermitian transpose, and λ is the regularization parameter. The regularized pressure is then $p_\lambda(\mathbf{r}) = \mathbf{a}_\lambda^T \boldsymbol{\alpha}(\mathbf{r})$. There are infinitely many columns in \mathbf{A} and elements in $\boldsymbol{\alpha}(\mathbf{r})$, and following [3] it is more convenient to use the expression

$$p_\lambda(\mathbf{r}) = \mathbf{p}^T (\mathbf{A} \mathbf{A}^H + \lambda^2 \mathbf{I})^{-1} \mathbf{A} \boldsymbol{\alpha}(\mathbf{r}). \quad (5)$$

The sums in each element of $\mathbf{A} \mathbf{A}^H$ and $\mathbf{A} \boldsymbol{\alpha}(\mathbf{r})$ represent integrals that are computed using numerical integration. To obtain the pressure and velocity on the source surface, the position \mathbf{r} is set accordingly in Eqs. (5) and (1).

ESM. The basic idea in ESM is to represent the radiation from the real sound source as a set of equivalent sources. In this paper, we use monopoles distributed near the physical source surface. Assuming that this model represents the radiated field, the pressure at the microphone positions can be expressed as in Eq. (2), but now element $\alpha_j(\mathbf{r})$ contains the free space Green's function from the position of the j th equivalent source to the point \mathbf{r} . As in SONAH, the coefficients (or source strengths) can be found by matching the field model to the measured data, and the solution is similar to that in Eq. (4), with a different coefficient matrix, of course.

In SONAH the wave expansion is continuous yielding matrices/vectors with infinite dimensions, but in ESM we have a finite number of equivalent sources, and the coefficient vector can therefore be computed explicitly. After the calculation of the coefficients via Eq. (4), the pressure and velocity are found using Eqs. (2) and (1).

IBEM. The direct BEM formulation is based on the Helmholtz integral equation. The boundary is discretized into an element mesh, and the pressure at a set

of field points can then be expressed as

$$\mathbf{p} = \mathbf{A}_m \mathbf{p}_s + \mathbf{B}_m \mathbf{v}_s, \quad (6)$$

where \mathbf{p}_s and \mathbf{v}_s contain the pressure and velocity at the nodes, respectively. Equation (6) can also be used to express the pressure in all the nodes:

$$\mathbf{p}_s = \mathbf{A}_s \mathbf{p}_s + \mathbf{B}_s \mathbf{v}_s, \quad (7)$$

Inserting Eq. (7) in Eq. (6) yields

$$\mathbf{p} = \mathbf{H} \mathbf{v}_s, \quad \mathbf{H} = \mathbf{A}_m (\mathbf{I} - \mathbf{A}_s)^{-1} \mathbf{B}_s + \mathbf{B}_m. \quad (8)$$

Equation (8) relates the velocity on the boundary of the sound source to the sound pressure at an arbitrary field point exterior to the source. For the inverse problem, the pressure \mathbf{p} is known, and \mathbf{v}_s is the unknown velocity which can be estimated using Tikhonov regularization as

$$\mathbf{v}_{s,\lambda} = (\mathbf{H}^H \mathbf{H} + \lambda^2 \mathbf{I})^{-1} \mathbf{H}^H \mathbf{p}. \quad (9)$$

Note that in IBEM the transfer matrix directly relates the field pressure to the surface velocity via Eq. (8), whereas in SONAH and ESM the transfer matrix relates the field pressure to wave coefficients via Eq. (3). This means that in IBEM, the PCM operates with a solution vector which is the physical quantity of interest (the particle velocity). In SONAH and ESM, however, after finding a regularization parameter the solution vector is multiplied by a matrix, cf. Eq. (2). This additional matrix multiplication in SONAH and ESM can be expected to have an additional smoothing effect on the solution.

2.2 The Parameter Choice Methods

Here we briefly summarize the three PCMs used in this work; we refer to [4] and [5] for details and further references. For all three NAH methods we use a common notation where \mathbf{p} denotes the measured data, \mathbf{K} is the coefficient/system matrix, and \mathbf{x}_λ is the regularized solution (either the coefficient vector \mathbf{a}_λ in SONAH and ESM, or the velocity vector $\mathbf{v}_{s,\lambda}$ in IBEM).

GCV is a statistically based method that seeks to minimize the prediction error $\|\mathbf{p}^t - \mathbf{K} \mathbf{x}_\lambda\|_2$ between the exact sound pressure \mathbf{p}^t and the predicted sound pressure. This is achieved by minimizing the GCV function:

$$\|\mathbf{p} - \mathbf{K} \mathbf{x}_\lambda\|_2 / \text{trace}(\mathbf{I} - \mathbf{K} (\mathbf{K}^H \mathbf{K} + \lambda^2 \mathbf{I})^{-1} \mathbf{K}^H).$$

The trace-term can easily be computed from the eigenvalue decomposition of the matrix $\mathbf{A} \mathbf{A}^H$ in SONAH, or an SVD of \mathbf{A} in ESM and \mathbf{H} in IBEM.

L-C is a heuristic method based on the L-curve, i.e., a log-log plot of the solution norm $\|\mathbf{x}_\lambda\|_2$ versus the residual norm $\|\mathbf{p} - \mathbf{K} \mathbf{x}_\lambda\|_2$. If this curve has the form of an “L” then the regularization parameter that corresponds to the corner of the “L” is often a good choice that balances the regularization and perturbation errors in the solution.

NCP is a new statistically based method that seeks to choose λ such that precisely all information is extracted from the data, and only noise is left in the residual. This is done via the normalized cumulative periodogram which is used to choose the λ for which the residual vector – in a statistical setting – can be considered “closest” to being white noise.

3 Simulation Results

In our simulations the measurement points are distributed in a regular grid of 8×8 points separated by 3 cm, with its center at $(x, y, z) = (0, 0, 0)$ m. The reconstruction points are at $z = -0.03$ m with the same x, y -coordinates as the measurement points. Two monopoles are placed at $\mathbf{r}_{s1} = (-0.05, 0.05, -0.06)$ m and $\mathbf{r}_{s2} = (0.08, 0, -0.06)$ m, respectively, to simulate a sound field.

Only the particle velocity in the z -direction is considered when calculating the reconstruction errors. As an error measure we use

$$\frac{\|\mathbf{v}_s - \mathbf{v}_{s,\lambda}\|_2}{\|\mathbf{v}_s\|_2} \times 100\%, \quad (10)$$

where the vectors \mathbf{v}_s and $\mathbf{v}_{s,\lambda}$ represent the true and estimated particle velocities, respectively.

To simulate measurement noise, phase mismatch between the microphones is introduced as $p_i = p_i^t \exp(j\phi_i)$, where p_i^t is the true sound pressure at the i th measurement position, and ϕ_i is the associated phase error taken from a uniform distribution with standard deviation 1° .

In SONAH one must set a virtual source plane, at which the evanescent components in the wave expansion has the same amplitude as the plane waves [3], and here this plane is located at $z = -0.075$ m. The equivalent sources in ESM are positioned at $z = -0.09$ m in 12×12 grid points centered around $(x, y) = (0, 0)$ m and with 3 cm separation. The boundary mesh in IBEM consists of 0.015×0.015 m quadratic elements that constitute a rectangular box of dimensions $0.33 \times 0.33 \times 0.12$ m surrounding the monopoles. The top side of this box coincides with the reconstruction surface, and it has nodes at the reconstruction points.

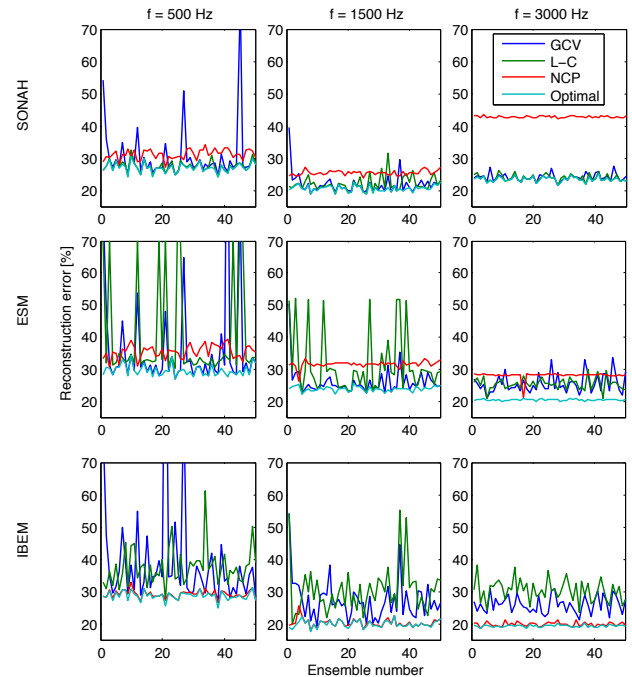


Figure 1: Reconstruction errors for 50 ensembles of simulated microphone mismatch for each frequency.

The phase error’s standard deviation is 1° .

The errors in the reconstructed velocities are shown in Fig. 1 for 50 sets of noise ensembles at three different

frequencies. Each plot shows the results using GCV, L-C, and NCP. The curves labelled “Optimal” correspond to the value of λ yielding the lowest smallest error for that given noise ensemble.

For SONAH the L-C and GCV methods generally yield lower errors than NCP, and the parameter choice is very close to the optimal choice. For GCV, however, there are a few outliers for $f = 500$ Hz. The behavior is more or less the same for ESM, except L-C has more outliers than GCV here.

During the simulations it was observed that for some noise ensembles the L-curve had two corners, and for some of these instances the “wrong” one was chosen – this is seen as errors around 50 % at $f = 1500$ Hz for ESM. For IBEM the better choice is clearly made by NCP, while both L-C and GCV are unstable and led to large errors. Notice that for all three methods NCP is generally stable in its parameter choice with respect to the ensembles, although having a higher error level.

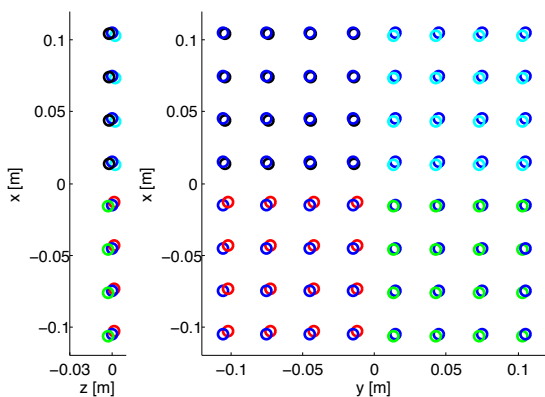


Figure 2: Microphone positions seen in the x, z -plane (left) and x, y -plane (right) before and after introducing misalignment. The blue circles are without misalignment and the other colors indicate four groups that are misaligned.

Next, misalignment of the microphones is simulated. The 64 microphones are divided into four groups, and the individual groups are displaced as shown in Fig. 2. The sound pressure at the misaligned points is used as measured pressure, but maintaining the original positions as the “assumed” positions in the reconstruction model. The noise ensembles from the previous simulation are reused in addition to the misaligned input data.

The reconstruction errors are shown in Fig. 3; notice that the vertical axis is different from that in Fig. 1. GCV is clearly significantly affected by the misalignment for all three methods, while L-C and NCP generally remain stable. A random misalignment of each individual microphone would serve as additional random phase mismatch, hence it is reasonable to believe that such a displacement would not affect the performance of GCV in the same way. Moving the entire array in the measurement plane, or turning it a few degrees around its own axis, did not introduce such large errors for GCV (results not shown here), but only a small misalignment of just one of the four groups in Fig. 2 was enough to provoke its instability.

These observations indicate that if a 4×4 array is used in practice to measure the pressure at the 64 posi-

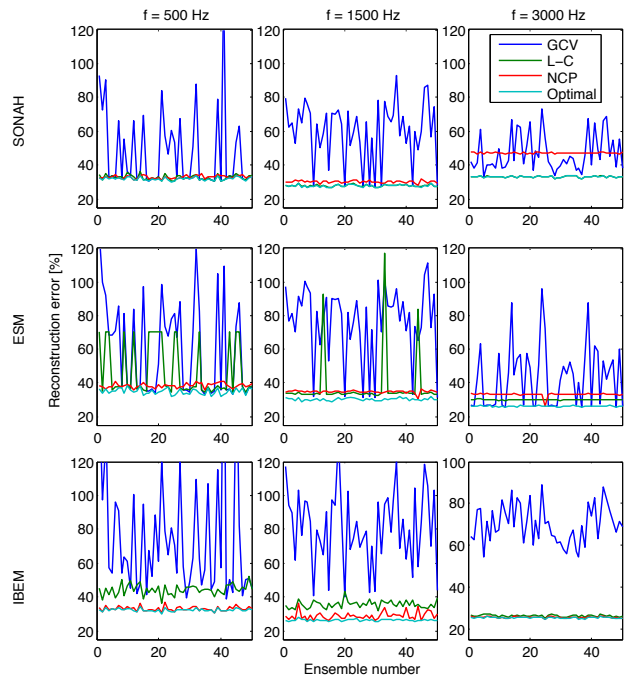


Figure 3: Reconstruction errors using the same noise ensembles as in Fig. 1, but with additional simulated misalignment of the microphones.

tions, there is a significant risk of getting low accuracy if GCV is used, compared to using an 8×8 array.

4 Experimental Results

Our experiments were carried out in an anechoic chamber using a source object consisting of a $0.4 \times 0.5 \times 0.4$ m box of 19-mm fibreboard with one side replaced by a 3-mm steel plate. The 0.4×0.5 m steel plate was excited near its center with broad-band noise using a Brüel & Kjær exciter. A stinger was mounted on the exciter, and a force transducer connected the stinger to the plate (using beeswax on the transducer).

The resulting normal velocity of the plate was measured in 16×14 points (with a 3 cm spacing between the points) using an Ometron laser vibrometer. The sound pressure was then measured at different positions with an 8×8 microphone array. First, it was positioned at the center position (symmetrically with respect to the plate), and then at four different positions yielding 16×16 measurement points (also symmetrically with respect to the plate). This was done at different standoff distances from the plate.

As in the previous section only the velocity reconstruction is considered, and to circumvent problems such as drift in the setup the transfer functions (between force transducer and laser/microphones) are used instead of the velocity itself. The results from the laser are assumed to be the “true” velocity and the error is calculated as in Eq. (10). However, since the difference in phase response between the laser and the microphones is unknown, only absolute values are considered when calculating the error.

The mesh used for IBEM consists of quadrilateral elements with 15 mm side lengths on the surface of the steel plate and approximately 30 mm on the remaining

sides of the box. In ESM the monopoles are distributed at a distance equal to 1.5 times the microphone spacing (45 mm) behind the plate. There is one monopole below each reconstruction point, and there are two additional rims of monopoles extending the region of equivalent sources, i.e., when reconstructing only at the 8×8 center points there are 12×12 monopoles, and when reconstructing at all 16×14 points there are 20×18 monopoles. In SONAH the virtual source plane is also placed 45 mm behind the plate.

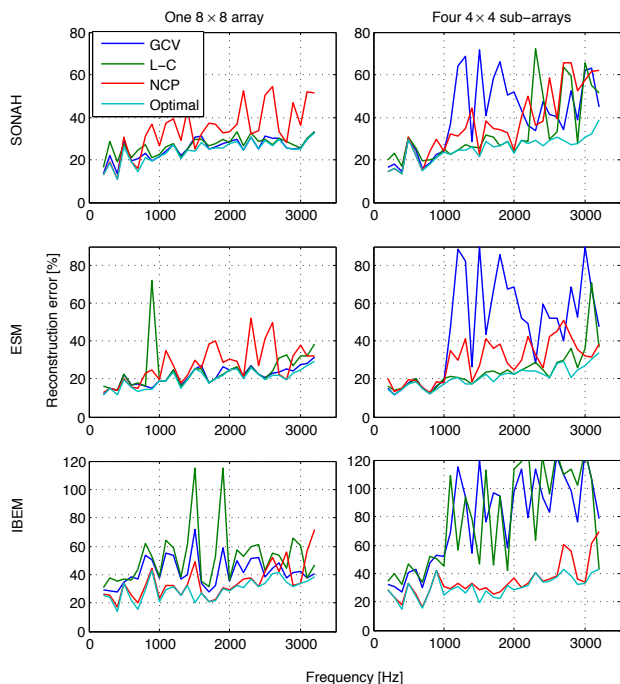


Figure 4: Reconstruction errors using data from 8×8 microphone positions around the center of the steel plate (standoff distance is 30 mm). Left: data from a single array. Right: data from four 4×4 sub-arrays.

Figure 4 shows the reconstruction errors versus frequency. The left column shows results based on data from a single 8×8 microphone array at the center. The results in the right column were obtained using four 4×4 sub-arrays from the 16×16 measurements, combined to yield a situation similar to that in Fig. 2. In both cases, there are 8×8 reconstructions points on the plate.

For GCV, the error clearly increases when using the four sub-arrays, while the error for L-C and NCP is more or less the same (at least for SONAH and ESM). Assuming that the main source of errors is the misalignment, these results are in agreement with our simulations. In SONAH and ESM, GCV is slightly better than L-C when using a single array, and NCP clearly produces larger errors. When combining the four sub-arrays, L-C is the better choice. In IBEM the highest accuracy is achieved with NCP for both cases and, as in the simulations, L-C and GCV do not work well.

In Fig. 5 all 16×16 measurements from the four arrays are used, and now the number of reconstruction points is increased to all the 16×14 points on the plate. For SONAH and ESM, the large misalignment errors for GCV are not seen here. We recall that the plots represent standoff distances different from that in Fig. 4, and part of the explanation for the better GCV results in

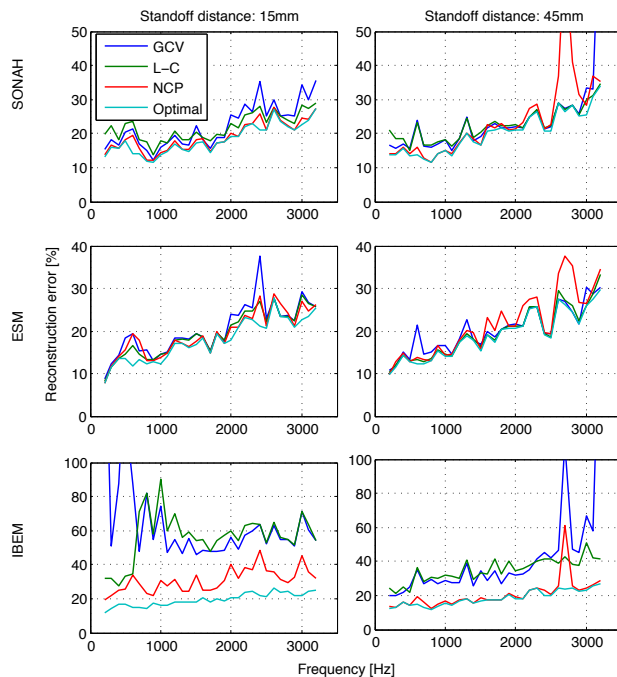


Figure 5: Reconstructed errors using the 16×16 measurements at two standoff distances.

Fig. 5 (for SONAH and ESM) could be that the array positions were better aligned for the 15 mm and 45 mm distances. However, when using the 16×16 measurements for the 30 mm distance the performance of GCV (not shown here) is better than in Fig. 4. When all 16×16 measurements are included, the 8×8 aligned points in the array cover a larger area in space than the 4×4 points from before, and hence it is fair to believe that the influence of misalignment decreases.

For SONAH and ESM the performance does not change much when increasing the standoff distance to 45 mm. This is, of course, not a general tendency for all sound sources. For example, a thinner steel plate would result in more evanescent waves components, and in such cases the standoff distance becomes more important. In IBEM the PCMs clearly perform better for the 45 mm distance.

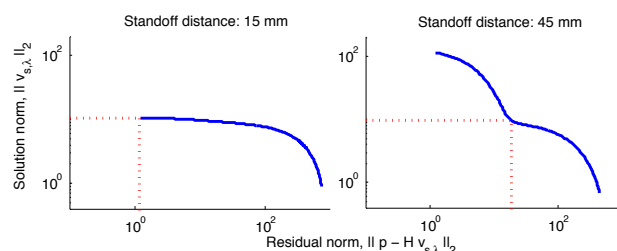


Figure 6: L-curves in IBEM for two different standoff distances at $f = 800$ Hz.

Figure 6 shows the L-curve in IBEM at $f = 800$ Hz for the two standoff distances. At 15 mm the curve has no L-shape, and the algorithm simply chooses the parameter corresponding to the smallest residual norm. As explained in Sec. 2.2 the L-curve criterion assumes that for a noisy ill-posed problem the solution norm increases dramatically when λ decreases beyond a certain level, and the more ill conditioned the problem the faster

the solution norm will increase. Normally, the lack of an L-shape means that no regularization is needed. However, as seen in the error for the 15 mm standoff (Fig. 5), some regularization is indeed required. The explanation for the missing L-shape is that the IBEM problem is well conditioned (from the point of perturbation analysis), which means the assumption behind the L-curve criterion is violated. When moving the measurement plane to 45 mm the problem becomes more ill conditioned which benefits the underlying requirements. Another way of making the problem more ill conditioned would be to increase the mesh density for the reconstruction, thereby including higher spatial frequencies in the source model. These high spatial frequencies represent strongly decaying wave components, which will translate into a more ill-posed problem.

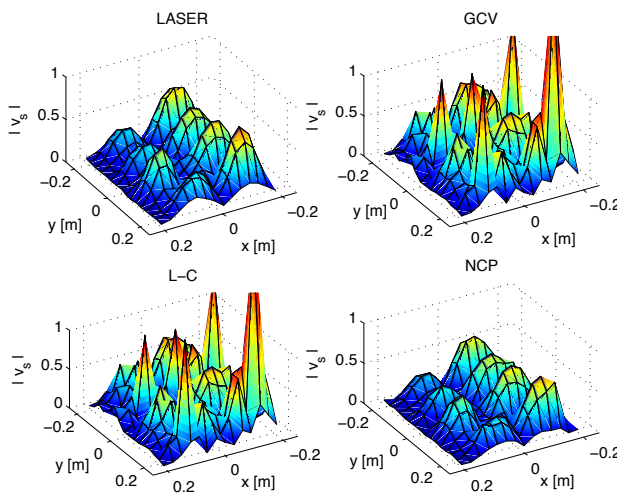


Figure 7: Absolute values of the reconstructed velocity in (m/s)/N on the steel plate, at $f = 800$ Hz using IBEM.

Figure 7 shows IBEM's predicted velocity distributions at $f = 800$ Hz for the 15 mm standoff. The very small regularization parameter selected by L-C and GCV results in a very noisy reconstruction, while NCP gives a good reconstruction. It is clearly seen that Tikhonov regularization has a filtering effect on the solution, which is crucial in order to get a meaningful solution – even when the L-curve seems to indicate that the problem is well conditioned.

5 Conclusion

Three parameter-choice methods (GCV, L-curve, and NCP) were compared for three different methods in near-field acoustical holography: SONAH, ESM, and IBEM. Our results show that GCV is sensitive to misalignment of the array positions when several array positions are used in one reconstruction. This effect is most severe when using combinations of smaller sub-arrays, e.g., with four arrays 4×4 microphones.

For SONAH and ESM the most robust method was the L-curve, while NCP in general gave higher errors. It was shown that an IBEM problem may be too well-conditioned for the parameter choice methods to select an appropriate regularization parameter. In such cases

it may be necessary to move further away from the source or refine the density of the boundary mesh. The best choice for IBEM was NCP, since GCV and the L-curve generally under-regularized the solution resulting in a noisy reconstruction.

The IBEM transfer matrix used in this paper directly relates the field pressure to the surface velocity, whereas in SONAH and ESM the transfer matrix relates the pressure to coefficients of elementary wave functions. Hence, in the latter, after finding a regularization parameter the resulting coefficients are multiplied by a matrix to get the velocity at the surface. This matrix multiplication has an additional smoothing effect, which may explain why GCV and the L-curve work better with SONAH and ESM, i.e., under-regularization by GCV and the L-curve yields good regularization after the additional “smoothing” matrix multiplication.

References

- [1] M. R. Bai, “Application of BEM (Boundary Element Method)-based acoustic holography to radiation analysis of sound sources with arbitrarily shaped geometries,” *J. Acoust. Soc. Am.* **92**, 533–549 (1992).
- [2] J. Gomes, “Comparing parameter choice methods for the regularization in the SONAH algorithm,” in *Proc. of Euro-Noise 2006*, Tampere, Finland (2006).
- [3] J. Hald and J. Gomes, “A comparison of two patch methods,” in *Proceedings of Inter-Noise 2006*, Honolulu, Hawaii (2006).
- [4] P. C. Hansen, *Rank-Deficient and Discrete Ill-Posed Problems: Numerical Aspects of Linear Inversion*, SIAM, Philadelphia (1997).
- [5] P. C. Hansen, M. E. Kilmer and R. H. Kjeldsen “Exploiting residual information in the parameter choice for discrete ill-posed problems,” *BIT* **46**, 41–59 (2006).
- [6] A. Sarkissian, “Method of superposition applied to pathc near-field acoustic holography,” *J. Acoust. Soc. Am.* **118**, 671–678 (2005).
- [7] A. Schuhmacher, J. Hald, K. B. Rasmussen and P. C. Hansen, “Sound source reconstruction using inverse boundary element calculations,” *J. Acoust. Soc. Am.* **113**, 114–127 (2003).
- [8] R. Steiner and J. Hald, “Near-field acoustical holography without the errors and limitations caused by the use of spatial DFT,” *International Journal of Acoustics and Vibration* **6**, 83–89 (2001).
- [9] E. G. Williams, “Regularization methods for near-field acoustical holography,” *J. Acoust. Soc. Am.* **110**, 1976–1988 (2001).